Modelling and Simulation of Direct Self-Control Systems*

K. L. SHI, T. F. CHAN, Y. K. WONG and S. L. HO
*Department of Electrical Engineering, The Hong Kong Polytechnic University, Hung Hom, Kowloon,
Hong Kong. E-mail: eetfchan@inet.polyu.edu.hk*

This paper describes a generalized model of the three-phase induction motor and simulation of the direct self-control (DSC) system, using the Matlab Simulink software. The advantage of Simulink modelling is that program compilation is not required. Instead, the mouse and Simulink menu commands are used to link the basic function blocks to yield the complete DSC system simulation model. This paper also shows the techniques to simplify and solve high-order and nonlinear equations in the design of the DSC system. It is also demonstrated that the DSC method is sensitive to the current sensor noise and the controller time delay.

SUMMARY OF THE EDUCATIONAL ASPECTS OF THIS PAPER

1. The paper describes software/hardware/simulation tools suitable for students of the following courses: Industrial Drives; Electrical Machines and Drives.
2. Level of students involved in the use of the materials: Industrial Drives (MSc); Electrical Machines and Drives (EEBENG degree, Year 3).
3. Aspects which are new include: application of Matlab *Simulink* for modelling an induction motor and direct self-controlled inverter-fed induction motor drive.
4. The material presented could form part of the lecture presentation of simulation of electric drives. Students could thus familiarise themselves with state-of-the-art software suitable for modelling and dynamic analysis of electric machines and drives.
5. The following texts accompany the presented materials: *Power Electric Control of AC Motors*, by Murphy and Turnbull, Pergamon Press; the paper, Direct self-control (DSC) of inverter-fed induction machines, by M. Depenbrock, *IEEE Transactions on Power Electronics*, **PE-3**(4), 1988, pp. 402–429.
6. The concepts presented have been tested in the classroom. One of the authors (T. F. Chan) incorporated the induction modelling part of the materials in the paper in the Industrial Drives course that he taught in Semester 1, 2001.
7. Using the block diagram approach of Matlab *Simulink*, the authors have demonstrated that a complicated engineering system (the induction motor and direct self-control induction motor system) can be modelled to yield the dynamic

performance, with much reduced programming effort. This approach could be extended to other engineering systems.

LIST OF SYMBOLS

L_s	stator inductance
L_m	mutual inductance
L_r	rotor inductance
R_s	stator resistance
R_r	rotor resistance
ω_o	rotor speed
P	pole number
V_{ds}, V_{qs}	d-axis and q-axis components of the stator voltage vector V_s
V_{dr}, V_{qr}	d-axis and q-axis components of the rotor voltage vector V_r
i_{ds}, i_{qs}	d-axis and q-axis components of the stator current vectors i_s
i_{dr}, i_{qr}	d-axis and q-axis components of the rotor current vectors i_r
ψ_{ds}, ψ_{qs}	d-axis and q-axis components of the primary flux vectors ψ_s
J	moment of inertia of rotor
J_L	moment of inertia of load

INTRODUCTION

THE DIRECT SELF-CONTROL (DSC) method [1–3] makes it possible to achieve precise control of torque and speed in an inverter-fed induction motor drive system. It is well suited to high-power drives with low switching frequency [1]. Evaluation of the direct self-control system can be performed in two ways. The first approach uses a real motor with an inverter and a DSC controller. Disadvantages of the practical approach are that it is difficult to observe and change the electrical parameters of the machine, the controller

time delay, or the sensor noise. The second approach uses a computer simulation of the system, witch can make up the disadvantages of the practical approach. In the computer simulation environment, all quantities can be readily observed and the parameters can be altered to investigate their effect on the system, thereby providing useful information for controller design. In addition, process noise, sensor noise, and different controller time delays can be added to simulate the actual performance.

Simulation of the three-phase induction machine is well documented in the literature and digital computer solutions can be performed using various methods, such as numeric programming [4, 5] and the electromagnetic transient program (EMTP) [6]. This paper discusses the use of the *Simulink* software of Matlab in the dynamic modelling of the induction motor and DSC simulation. The main advantage of *Simulink* over other programming softwares is that, instead of compilation of program code, the simulation model is built up systematically by means of basic function blocks. A set of machine differential equations can thus be modelled by interconnection of appropriate function blocks, each of which performing a specific mathematical operation. Programming efforts are drastically reduced and the debugging of errors is easy. Since *Simulink* is a model operation programmer, the induction motor model and DSC model can be easily linked to form the complete direct self-control system.

GENERALISED MODEL OF THE INDUCTION MOTOR

A generalised dynamic model of the induction motor consists of:

1. an electrical sub-model to implement the three-phase to two-axis (3/2) transformation of stator voltage and current;
2. a torque sub-model to calculate the developed torque;
3. a mechanical sub-model to yield the rotor speed.

Electrical sub-model of the induction motor

The three-phase to two-axis voltage transformation is given by the following matrix equation [7]:

$$\begin{bmatrix} V_{ds} \\ V_{qs} \end{bmatrix} = \underbrace{\begin{bmatrix} 1 & -1/2 & -1/2 \\ 0 & \sqrt{3}/2 & -\sqrt{3}/2 \end{bmatrix}}_{[A]} \begin{bmatrix} V_{as} \\ V_{bs} \\ V_{cs} \end{bmatrix} \quad (1)$$

where V_{as}, V_{bs}, and V_{cs} are the three-phase stator voltages, while V_{ds} and V_{qs} are the two-axis components of the stator voltage vector V_s.

Using vector notation, the electrical model can be expressed in the two-axis stator reference frame.

The voltage equation of an induction motor can be written as [7]:

$$\begin{bmatrix} V_{ds} \\ V_{qs} \\ V_{dr} \\ V_{qr} \end{bmatrix}$$

$$= \begin{bmatrix} R_s & 0 & 0 & 0 \\ 0 & R_s & 0 & 0 \\ 0 & \frac{P}{2}\omega_o L_m & R_r & \frac{P}{2}\omega_o L_r \\ -\frac{P}{2}\omega_o L_m & 0 & -\frac{P}{2}\omega_o L_r & R_r \end{bmatrix} \begin{bmatrix} i_{ds} \\ i_{qs} \\ i_{dr} \\ i_{qr} \end{bmatrix}$$

$$+ \begin{bmatrix} L_s & 0 & L_m & 0 \\ 0 & L_s & 0 & L_m \\ L_m & 0 & L_r & 0 \\ 0 & L_m & 0 & L_r \end{bmatrix} * \frac{d}{dt} \begin{bmatrix} i_{ds} \\ i_{qs} \\ i_{dr} \\ i_{qr} \end{bmatrix} \quad (2)$$

The equation for computing the current vector may be derived from Equation (2).

$$\begin{bmatrix} i_{ds} \\ i_{qs} \\ i_{dr} \\ i_{qr} \end{bmatrix} = \int_{\tau=0}^{t} \left\{ \underbrace{\begin{bmatrix} L_s & 0 & L_m & 0 \\ 0 & L_s & 0 & L_m \\ L_m & 0 & L_r & 0 \\ 0 & L_m & 0 & L_r \end{bmatrix}^{-1}}_{[B]} \left(\begin{bmatrix} V_{ds} \\ V_{qs} \\ V_{dr} \\ V_{qr} \end{bmatrix} \right. \right.$$

$$- \underbrace{\begin{bmatrix} R_s & 0 & 0 & 0 \\ 0 & R_s & 0 & 0 \\ 0 & \frac{P}{2}\omega_o L_m & R_r & \frac{P}{2}\omega_o L_r \\ -\frac{P}{2}\omega_o L_m & 0 & -\frac{P}{2}\omega_o L_r & R_r \end{bmatrix}}_{[C]}$$

$$\left. \left. \times \begin{bmatrix} i_{ds} \\ i_{qs} \\ i_{dr} \\ i_{qr} \end{bmatrix} \right) \right\} d\tau \quad (3)$$

As shown in Fig.1, Matrix [A] in Equation (1) and matrix [B] in Equation (2) can be implemented by the 'Matrix Gain' block of *Simulink* [7], while matrix [C] in Equation (2) can be implemented by four 'Fcn' blocks of SIMULINK whose detail is illustrated in Fig. 2.

In the electrical model, the three-phase voltage $[V_{as}, V_{bs}, V_{cs}]$ is the input and the current vector $[i_{ds}, i_{qs}, i_{dr}, i_{qr}]$ is the output vector. The rotor voltage vector is normally zero because of the short-circuited cage rotor winding, i.e., $V_{dr}=0$ and $V_{qr}=0$.
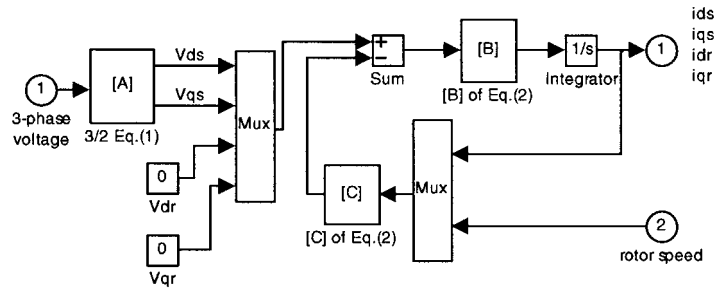
Fig. 1. Electrical model of an induction motor in *Simulink*.

Torque sub-model of induction motor

In the two-axis stator reference frame, the electro-magnetic *T* is given by [7]:

$$T = \frac{PL_m}{3}(i_{dr}i_{qs} - i_{qr}i_{ds}) \qquad (4)$$

Figure 3 shows how the torque sub-model is realized in *Simulink*.

Mechanical sub-model of induction motor

Neglecting viscous friction torque and using the torque balance equation, the rotor speed ω_o may be calculated as follows:

$$\omega_o = \int_{\tau=0}^{t} \frac{T - T_L}{J} d\tau \qquad (5)$$

Figure 4 shows the mechanical sub-model based on Equation (5).

The electrical sub-model in Fig. 1, the torque sub-model in Fig. 3, and the mechanical sub-model in Fig. 4 are grouped together to form the induction motor model as shown in Fig. 5. The two 'Scope' blocks enable the speed and torque of the motor to be observed.

SIMULATION OF AN INDUCTION MOTOR

The squirrel-cage induction motor chosen for the simulation studies has the following parameters:

- three-phase, 7.5 kW
- 6-pole, Y-connected
- $R_s = 0.288\,\Omega/\text{ph}$

- $R_r = 0.158\,\Omega/\text{ph}$
- $L_s = 0.0425\,\Omega/\text{ph}$
- $L_m = 0.0412\,\Omega/\text{ph}$
- $L_r = 0.0418\,\Omega/\text{ph}$
- $J = 0.4\,\text{kg.m}^2$
- $J_L = 0.4\,\text{kg.m}^2$

To illustrate an application of the induction motor model, a simulation study of direct-on-line starting is carried out. At $t = 0$, the motor, previously de-energized and at standstill, is connected to a 220 V, 60 Hz supply. The power source is constructed using a signal generator block from the *Simulink* library. The load torque, T_L, is assumed to be 20 N.m, and independent of speed. Figure 6 shows the results of computer simulation, which are similar to those obtained using the classical numeric programming approach.

MODELLING OF DIRECT SELF-CONTROL

The direct self-control method gives an inverter-fed induction motor an excellent dynamic performance. In this drive system, the instantaneous control principle of the torque and the primary flux is based on hysteresis comparisons by selecting the optimum inverter switching modes [2]. In this paper, a direct self-controller is modelled using *Simulink* in order to investigate the effect of the non-zero mean value noise of the current sensor on the torque and speed responses of induction motor. The *Simulink* model of the direct self-controller consists of:
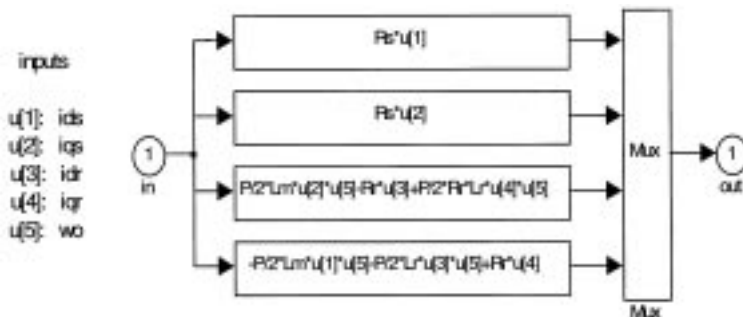
- the flux calculator;
- the torque calculator;

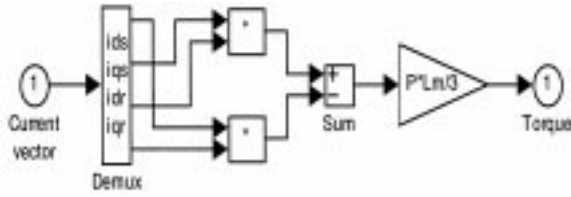Fig. 2. Matrix [C] implemented using four Fcn blocks of *Simulink*.
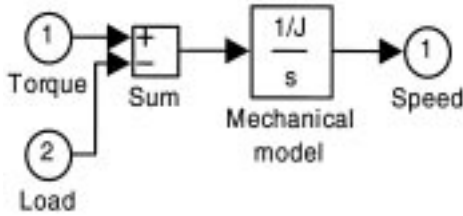
Fig. 3. Torque sub-model.

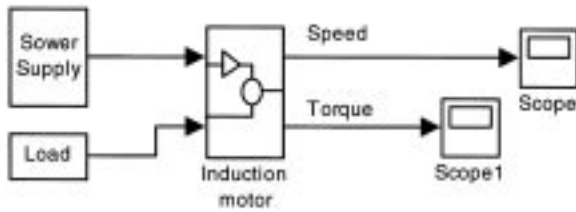Fig. 4. Mechanical sub-model in *Simulink* window.

Fig. 5. Induction motor simulation system.

- the flux and torque hysteresis comparator;
- the optimum voltage switching table;
- the voltage source inverter, as shown in Fig. 7.

Model of the flux calculator
   The primary flux vector model of the induction motor is expressed by [3]:

$$\psi = \int_{\tau=0}^{t} (V_s - R_s i_s)\, d\tau \qquad (6)$$

where $\psi = \psi_{ds} + j\psi_{qs}$.

Model of the torque calculator
   The instantaneous value of the electromagnetic torque is given by [7]:

$$T = \frac{P}{2}\frac{2}{3}(\psi_{ds}i_{qs} - \psi_{qs}i_{ds}) \qquad (7)$$

Model of flux and torque hysteresis comparator
   The model consists of the flux hysteresis comparator and torque hysteresis comparator. In the flux hysteresis comparator, the flux error between primary flux $|\psi|$ and its command $|\psi^*|$ can be limited within $\pm\Delta|\psi|$, as expressed in Equation (8), and the flux error code B_6 produced by the hysteresis comparator will be used to select
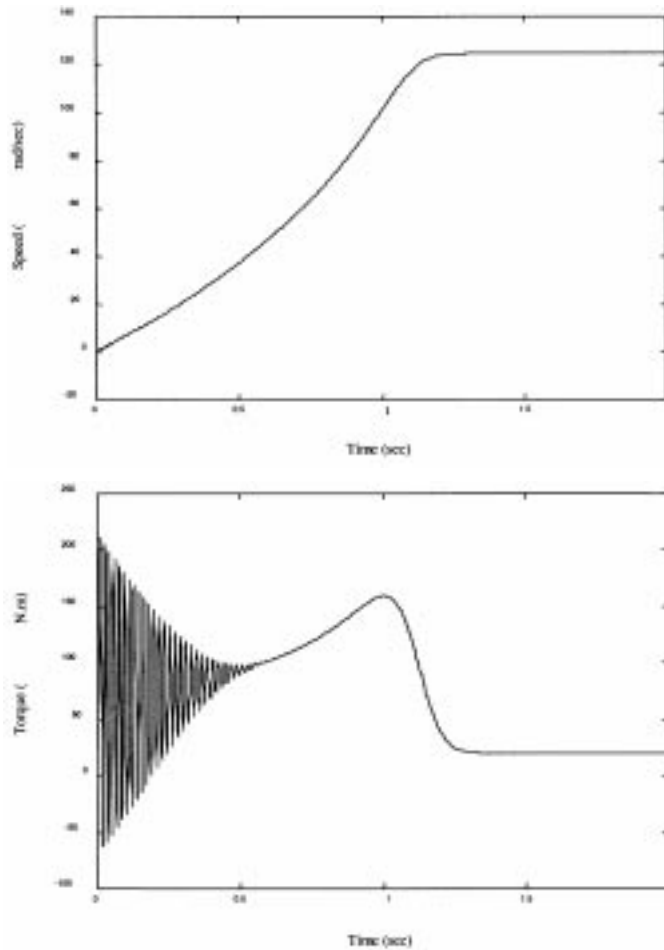

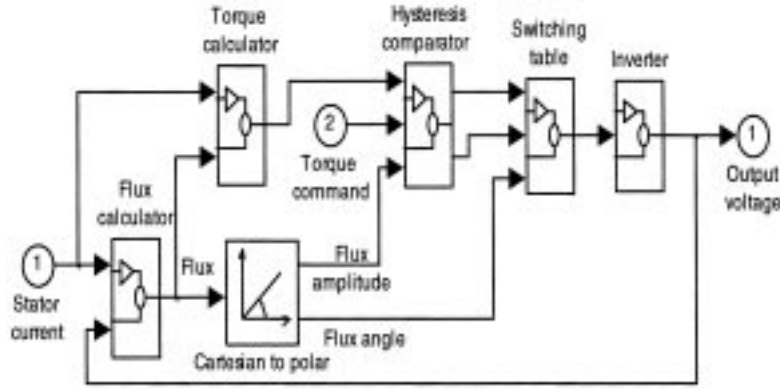Fig. 6. Speed and torque of the induction motor with direct-on-line staring.

Fig. 7. DSC controller blocks in *Simulink*.

the voltage space vector [2].

$$|\psi|^* - \Delta|\psi| \leq |\psi| \leq |\psi|^* + \Delta|\psi| \tag{8}$$

where $|\psi| = \sqrt{\psi_{ds}^2 + \psi_{qs}^2}$.

In the torque hysteresis comparator, the difference between the motor torque T and the torque command T^* is compared with ΔT and the error flag will produce a torque error code for selecting the voltage space vector, i.e.

$$T^* - \Delta T \leq T \leq T^* \tag{9}$$

(when ψ rotates in the clockwise direction)

$$T^* \leq T \leq T^* + \Delta T \tag{10}$$

(when ψ rotates in the counterclockwise direction).

As shown in Fig. 8, a 'relay' block of *Simulink* is used to implement the flux amplitude hysteresis comparator, while the other two 'relay' blocks and a 'sum' block implement the three-level torque hysteresis comparator.

Model of the optimum switching table

The space voltage vector is represented by eight different codes, two of which are the zero voltage codes (1, 1, 1) and (0, 0, 0), and the remaining are the six nonzero voltage codes, e.g., (1, 0, 0), . . . , (0, 1, 1). Similarly, the primary flux angle may be encoded as (1, 0, 0), . . . , (0, 1, 1), which represent six space positions of the flux vectors. In the DSC optimum switch table [2], the flux angle code $B_1 \sim B_3$, the torque error code $B_4 \sim B_5$, and the

flux error code B_6 together determine the optimum output voltage as shown in Table 1.

The optimum switching table (Table 1) is implemented by the 'combinatorial logic' block of *Simulink* as shown in Fig. 9.

In Fig . 9, the input is the flux amplitude error code B_6 from the flux hysteresis comparator in Fig. 8, the input ② is the torque error code $B_4 \sim B_5$ from the torque hysteresis comparator in Fig. 8, and the input ③ is the flux angle from the 'cartesian to polar' block in Fig. 7. The 'angle encode' block outputs the flux angle code $B_1 \sim B_3$, together with the torque error code $B_4 \sim B_5$ and the flux amplitude error code B_6 to form the input vector ($B_1 \sim B_6$) of the switch table block. The output of the 'combinatorial logic' block is the output voltage vectors, which is the input of the model of voltage inverter.

Model of the voltage inverter

The output voltage codes of the optimum switch table represent the status of the inverter switches. If the voltage code is denoted by (S_a, S_b, S_c), the space voltage vector V_s may be represented as [3]:

$$V_s = V_{ds} + jV_{qs} = |V_s|(S_a + S_b e^{j(2\pi/3)} + S_c e^{j(4\pi/3)}) \tag{11}$$

A 'combinatorial logic' block of *Simulink* is used to implement the voltage source inverter according to Equation (11), giving the desired voltage vector.
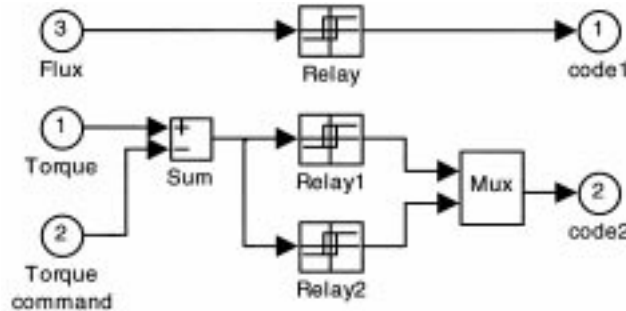

Fig. 8. Model of flux and torque hysteresis comparator in *Simulink*.

Table 1. DSC optimum switching table

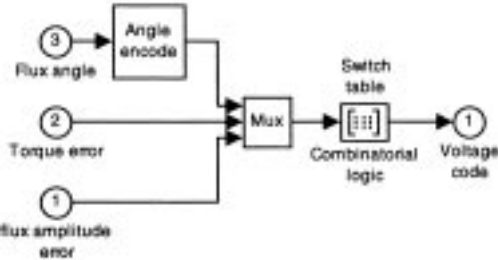| $V_s(S_a, S_b, S_c)$	$B_1 \sim B_3 = 001$	$B_1 \sim B_3 = 010$	$B_1 \sim B_3 = 011$	$B_1 \sim B_3 = 100$	$B_1 \sim B_3 = 101$	$B_1 \sim B_3 = 110$
$B_{456} = 010$	(0, 1, 1)	(1, 1, 0)	(0, 1, 0)	(1, 0, 1)	(0, 0, 1)	(1, 0, 0)
$B_{456} = 000$	(1, 1, 1)	(1, 1, 1)	(0, 0, 0)	(1, 1, 1)	(0, 0, 0)	(0, 0, 0)
$B_{456} = 100$	(1, 0, 1)	(0, 1, 1)	(0, 0, 1)	(1, 1, 0)	(1, 0, 0)	(0, 1, 0)
$B_{456} = 011$	(0, 1, 0)	(1, 0, 0)	(1, 1, 0)	(0, 0, 1)	(0, 1, 1)	(1, 0, 1)
$B_{456} = 001$	(0, 0, 0)	(0, 0, 0)	(1, 1, 1)	(0, 0, 0)	(1, 1, 1)	(1, 1, 1)
$B_{456} = 101$	(1, 0, 0)	(0, 0, 1)	(1, 0, 1)	(0, 1, 0)	(1, 1, 0)	(0, 1, 1)

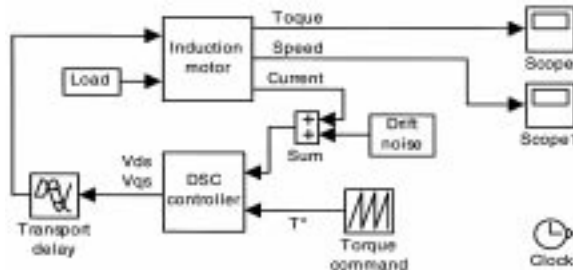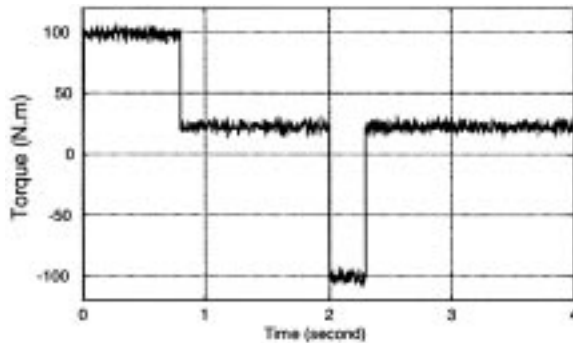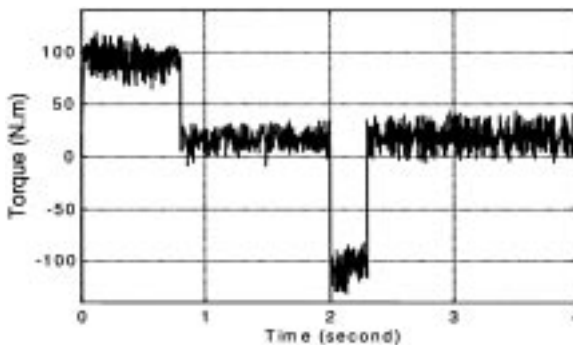Fig. 9. Model of optimum switching table in *Simulink*.

Fig. 10. DSC simulation blocks in *Simulink*.

Fig. 11. Torque response of DSC with controller delay 25 μs.

Fig. 12. Torque response of DSC with controller delay 100 μs.

SIMULATION OF DIRECT SELF-CONTROL SYSTEM

A complete simulation model of the DSC system is shown in Fig. 10. It consists of the induction motor model (the motor parameters and load are the same as those mentioned above), the DSC model, *Simulink* 'repeating sequence' block to produce the torque command, a 'transport delay' block for simulating the controller time delay, and a noise block to output the current drift noise. In addition, two 'scope' blocks are included to enable the torque and rotor speed to be observed. Two investigations were undertaken: 1) effects of the controller time delay and 2) effects of current sensor noise.

Effects of the controller time delay
As a predictive control scheme, the DSC has a steady-state control error produced by the time delay of the lengthy computation [1]. In this simulation, the flux and torque commands are as follows.

$$|\lambda_s|^* = 0.86 \, \text{Wb} \qquad 0 \, \text{s} < t \le 4 \, s$$
$$T^* = 100 \, (\text{N.m}) \qquad 0 \, \text{s} < t \le 0.8 \, s$$
$$T^* = 20 \, (\text{N.m}) \qquad 0.8 \, \text{s} < t \le 2 \, s$$
$$T^* = -100 \, (\text{N.m}) \qquad 2 \, \text{s} < t \le 2.3 \, s$$
$$T^* = 20 \, (\text{N.m}) \qquad 2.3 \, \text{s} < t \le 4 \, s$$

Figures 11, 13, and 15 show the torque response, flux response, and speed response of the DSC control system with 25 μs controller delay, while Figs 12, 14, and 16 show the simulation results of the DSC control system when the controller has 100 μs time delay. These results demonstrate that DSC is sensitive to the controller time delay and the torque and flux errors of DSC increase with increasing controller delay time. The large torque and flux errors will decrease the robustness of the DSC drive system against noise, although the speed response is relatively unaffected.

Effect of sensor noise on controller performance
Direct self-control depends on the definite integral calculation of the primary flux. When the cumulative flux error contributed by the definite integral exceeds a certain value, the wrong flux value will result in a control failure. When the control time is long, it is difficult to ensure that the system is free from noise sources of non-zero mean value [9]. Let i_s be the actual current and n be the
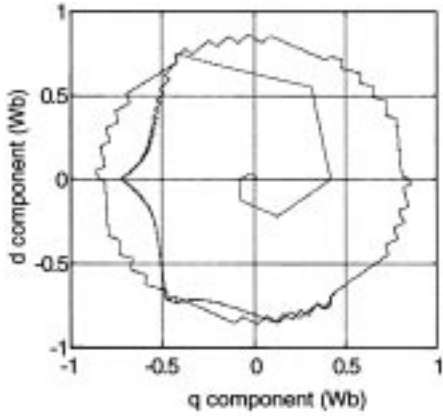
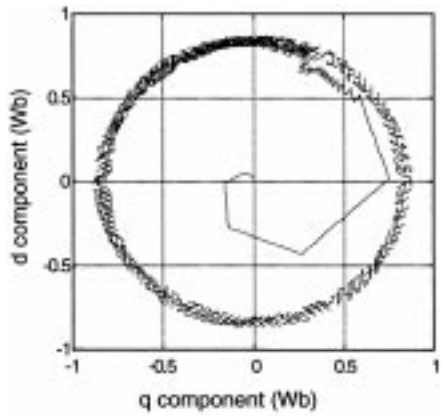Fig. 13. Primary flux Vector of DSC with controller delay $25\,\mu s$ (time $= 0\,s \sim 0.2\,s$).

Fig. 14. Primary flux Vector of DSC with controller delay $100\,\mu s$ (time $= 0\,s \sim 0.2\,s$).
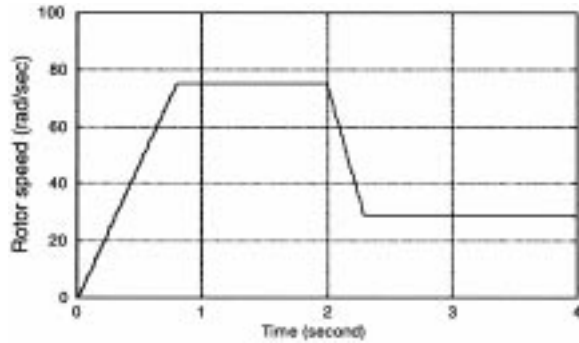
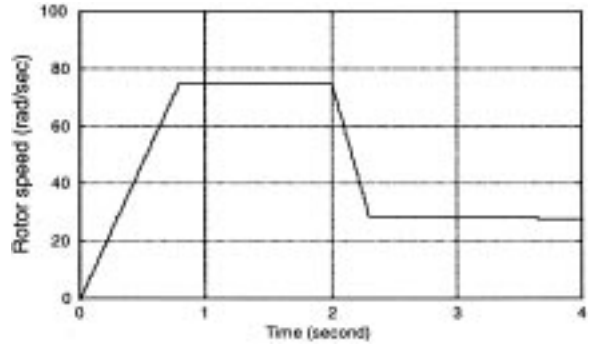Fig. 15. Rotor speed of DSC with controller delay $25\,\mu s$.
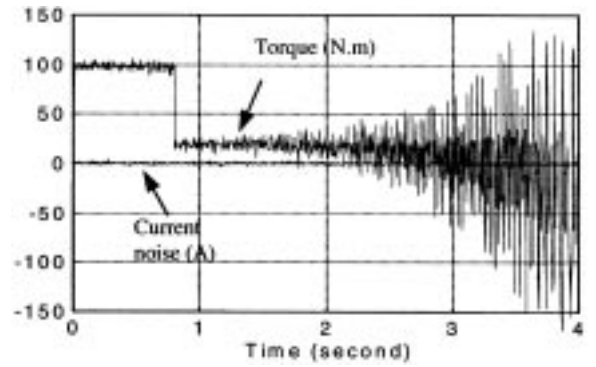

Fig. 16. Rotor speed of DSC with controller delay $100\,\mu s$.

Fig. 17. Torque of DSC controller with nonzero mean value noise.

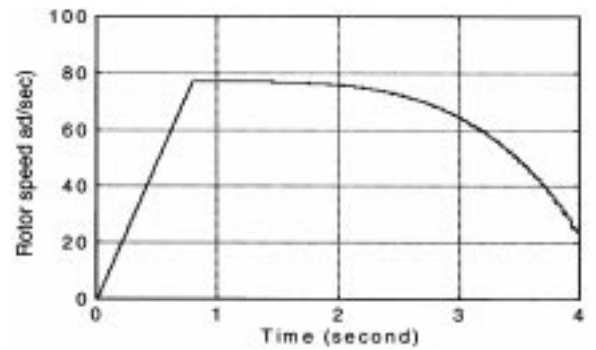Fig. 18. Speed of DSC controller with nonzero mean value noise.

sensor noise, then the current with noise $\tilde{i}_s$ is given by $\tilde{i}_s = i_s + n$. Substituting $\tilde{i}_s$ into Equation (6), the flux ψ is given by:

$$\psi = \int_{\tau=0}^{t} (V_s - R_s\tilde{i}_s)\, d\tau$$

$$= \int_{\tau=0}^{t} (V_s - R_si_s)\, d\tau - \int_{\tau=0}^{t} R_sn\, d\tau \quad (12)$$

Hence the flux error $\Delta\psi$ is given by:

$$\Delta\psi = - \int_{\tau=0}^{t} R_sn\, d\tau \quad (13)$$

When n has a nonzero mean value, the flux error $\Delta\psi$ will accumulate according to Equation (13). To demonstrate the effect of current sensor noise, a noise source is introduced into the actual current as shown in Fig. 10. It is assumed that the current sensor noise has a variance of 1 and its mean value drifts from $0\,A$ ($t = 0\,s$) to $1\,A$ ($t = 4\,s$) as shown in Fig. 17.

In this simulation, the controller time delay is assumed to be zero and the flux command is the

same as the first DSC simulation investigation, while the torque command is as follows:

$$T^* = 100\,(\text{N.m}) \quad 0\,\text{s} < t \leq 0.8\,\text{s}$$
$$T^* = 20\,(\text{N.m}) \quad 0.8\,\text{s} < t \leq 4\,\text{s}$$

The speed and torque responses in Figs 17 and 18 show that DSC is sensitive to noise with non-zero mean value. At $t = 4\,\text{s}$, the motor speed drops to 22 rad/sec and the control fails.

CONCLUSIONS

In this paper, the use of the Matlab *Simulink* software in modelling of the induction motor and the DSC system is described. Using *Simulink*, each block of the system model may be constructed and modified conveniently. Certain limit conditions, such as magnetic saturation and stator current limit, may be easily inserted in the function blocks. The fact that complex system models (such as the DSC system) can be simulated renders *Simulink* an ideal tool for the study of electric machine drives. The simulation results on DSC also reveal that the controllability of the system is affected by sensor noise, an important aspect that needs to be addressed when designing a practical drive system.

REFERENCES

1. T. G. Habetler, F. Profumo, M. Pastorelli, and L. M. Tolbert, Direct torque control of induction machines using space vector modulation, *IEEE Trans. Industry Application*, **IA-28**(5), 1992, pp. 1045–1053.
2. I. Takahashi and T. Noguchi, A new quick-response and high-efficiency control strategy of an induction motor, *IEEE Trans. Industry Application*, **IA-22**(5) 1986, pp. 820–827.
3. M. Depenbrock, Direct self-control (DSC) of inverter-fed induction machines, *IEEE Trans. Power Electronics*, **PE-3**(4) 1988, pp. 420–429.
4. S. N. Ghani, Digital computer simulation of three-phase induction machine dynamics—a generalized approach, *IEEE Trans. Industry Application*, **IA-24**(1), 1988, pp. 106–114.
5. E. Y. Y. Ho and P. C. Sen, Digital simulation of PWM induction motor drives for transient and steady-state performance, *IEEE Trans. Industrial Electronics*, **IE-33** (1), 1986, pp. 66–77.
6. A. Domijan, Jr, and Y. Yin, Single phase induction machine simulation using the electromagnetic transients program: theory and test cases, *Transaction on Energy Conversion*, **EC-9**(3), 1994, pp. 535–542.
7. A. M. Trzynadlowski, *The Field Orientation Principle in Control of Induction Motors*, KLUWER ACADEMIC PUBLISHERS (1994).
8. *Using SIMULINK, Dynamic System Simulation for MATLAB*, The MathWorks Inc. (1997).
9. J. Engberg and T. Larsen, *Noise Theory of Linear and Nonlinear Circuits*, John Wiley Sons Ltd., England (1995).

K. L. Shi received the B. Sc. degree from Chengdu University of Science and Technology (China) in 1983 and received a M. Sc. degree from Harbin Institute of Technology (China) in 1989, and the Ph. D. degree from the Hong Kong Polytechnic University (Hong Kong) in 2001. His current research interests are intelligent control and estimation of induction motor and permanent-magnet brushless DC motor drives.

T. F. Chan received the B. Sc.(Eng.) and M. Phil. degrees in electrical engineering from the University of Hong Kong, in 1974 and 1980. Since 1978, Mr. Chan has been with the Department of Electrical Engineering, the Hong Kong Polytechnic University, where he is now an associate Professor. His current research interests are self-excited AC generator, brushless AC generators and computer-aided design of electrical machines. Mr. Chan is also a member of the Institution of Electrical Engineers, London, U.K. and Hong Kong Institution of Engineers, Hong Kong.

Y. K. Wong received the B. Sc. and M. Sc. degree, Dip. Ed. from the London, the M. Soc. Sc. degree from the University of Hong Kong, the M. Phil. degree from the Chinese University of Hong Kong and the PhD degree from the Heriot-Watt University, UK. He joined the Hong Kong Polytechnic University in 1980. He is a Chartered Engineer, Chartered Mathematician, and Chartered Statistician. Dr. Wong is a Member of the IEE, Senior Member of the IEEE, Fellow of the Institute of Mathematics and its Applications and Fellow of the Royal Statistical Society. His current research interests include linear systems, modelling, simulation, intelligent control and power system control. He has written more than 100 articles published in international journals and conference proceedings.

S. L. Ho obtained his B. Sc. (First Class Honours) and Ph. D. degree in Electrical Engineering from the University of Warwick in 1976 and 1979. He joined the Department of Electrical Engineering, Hong Kong Polytechnic University in 1979. He is currently a full professor. S. L. Ho is very active in the areas of machine design, phantom loading of motors, condition monitoring of electrical machines and traction engineering. He has published more than 100 papers in international journals and conferences.